

DYNAMIC MODELING WITH CONDITIONAL QUANTILE TRAJECTORIES FOR LONGITUDINAL SNIPPET DATA, WITH APPLICATION TO COGNITIVE DECLINE OF ALZHEIMER'S PATIENTS^{†*}

Matthew Dawson¹ and Hans-Georg Müller²

¹ Graduate Group in Biostatistics, University of California, Davis

² Department of Statistics, University of California, Davis
Davis, CA 95616 USA

October 2016

ABSTRACT

Longitudinal data are often plagued with sparsity of time points where measurements are available. The functional data analysis perspective has been shown to provide an effective and flexible approach to address this problem for the case where measurements are sparse but their times are randomly distributed over an interval. Here we focus on a different scenario where available data can be characterized as snippets, which are very short stretches of longitudinal measurements. For each subject the stretch of available data is much shorter than the time frame of interest, a common occurrence in accelerated longitudinal studies. An added challenge is introduced if a time proxy that is basic for usual longitudinal modeling is not available. This situation arises in the case of Alzheimer's disease and comparable scenarios, where one is interested in time dynamics of declining performance, but the time of disease onset is unknown and the chronological age does not provide a meaningful time reference for longitudinal modeling. Our main methodological contribution is to address this problem with a novel approach. Key quantities for our approach are conditional quantile trajectories for monotonic processes that emerge as solutions of a dynamic system, and for which we obtain uniformly consistent estimates. These trajectories are shown to be useful to describe processes that quantify deterioration over time, such as hippocampal volumes in Alzheimer's patients.

KEY WORDS: Functional data analysis, accelerated longitudinal study, autonomous differential equations, uniform convergence, monotonic processes, nonparametric estimation, hippocampal volume.

[†] This research was supported by NSF grants DMS-1228369 and DMS-1407852.

^{*} The data used in this paper are from the Alzheimer's Disease Center at University of California Davis, supported by NIH and NIA grant P30 AG10129

1. INTRODUCTION

When adopting the functional approach for the analysis of longitudinal data, a common assumption is that the observations originate from a smooth underlying process. This assumption is justified, for example, when the observations correspond to biological mechanisms which are known to vary smoothly, and in this case modeling longitudinal data with functional data analysis (FDA) approaches has been highly successful (Brumback and Bracke 1998; Staniswalis et al. 1998; Rice and Wu 2001; Rice 2004; Guo 2004; Jiang and Wang 2011; Coffey et al. 2014; Wang 2003; Wang et al. 2005). A common methodological challenge in longitudinal studies, however, is that many such studies lack complete and densely spaced observations over time. Some authors have explored problems relating to incomplete functional data, for example Yao et al. (2005) focused on building a bridge between sparse longitudinal data and FDA; Kraus (2015) and Liebl and Kneip (2016) examined functional missingness in the case of otherwise dense data. While these methods are based on prediction of functional principal components, Delaigle and Hall (2013) constructed a functional classifier in the presence of overlapping but partially censored curve fragments. The methods of Delaigle and Hall involved an algorithm which stitches these fragments together, so there are two existing approaches for sparsely measured functional data that apply to very different sparseness scenarios, respectively.

In this paper, we consider a third approach for a type of sparseness that substantially differs from the ones considered previously. Some data generated in longitudinal studies exhibit an extreme form of sparseness and we refer to such data as snippet data, often originating from *accelerated longitudinal designs* (Galbraith et al. 2014). Such data can be characterized as very short longitudinal measurements relative to the domain of interest. A design of this type is attractive to practitioners across the social and life sciences since it minimizes the length of time over which one needs to gather data for each subject; they are especially useful in situations where data collection is invasive, difficult or expensive,

as is for example the case when studying Alzheimer’s disease.

Snippet data may be viewed as being generated by observing each subject for a short window around some random time T . An illustration of how snippets originate is shown in Figure 1.

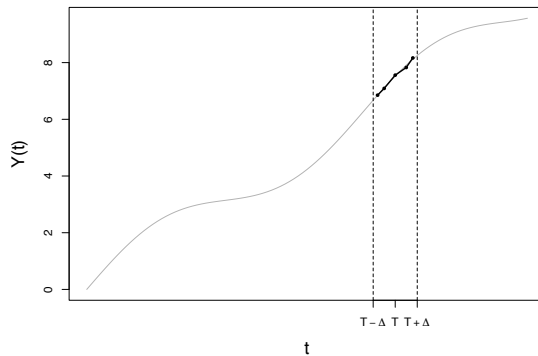


Figure 1: An example trajectory along with a longitudinal snippet at time T .

Typical methods for dealing with snippet data resulting from accelerated longitudinal studies involve parametric models (see for example (Raudenbush and Chan 1992; Ford et al. 2012; Baskin-Sommers et al. 2015; Stanik et al. 2013; Galla et al. 2014; Brault et al. 2011)). These methods do not allow the recovery of the underlying functional dynamics, which has not been systematically studied so far. The focus of this paper is to flexibly estimate quantile dynamics of the underlying smooth process, including cases where the subjects’ entry times T_i are not necessarily useful, a situation which arises when measuring deterioration since an unknown onset of disease or degradation in degradation experiments. Specifically, for snippet data where the absolute time scale is not informative, the functional completion method of Delaigle and Hall (2013) is not valid. The covariance function is also not estimable which also precludes the methods of Yao et al. (2005), Kraus (2015), and Liebl and Kneip (2016). Figure 2 demonstrates why the covariance function cannot be estimated in the snippet case, in contrast to the usually

considered sparse case where measurements are randomly located over the entire domain.

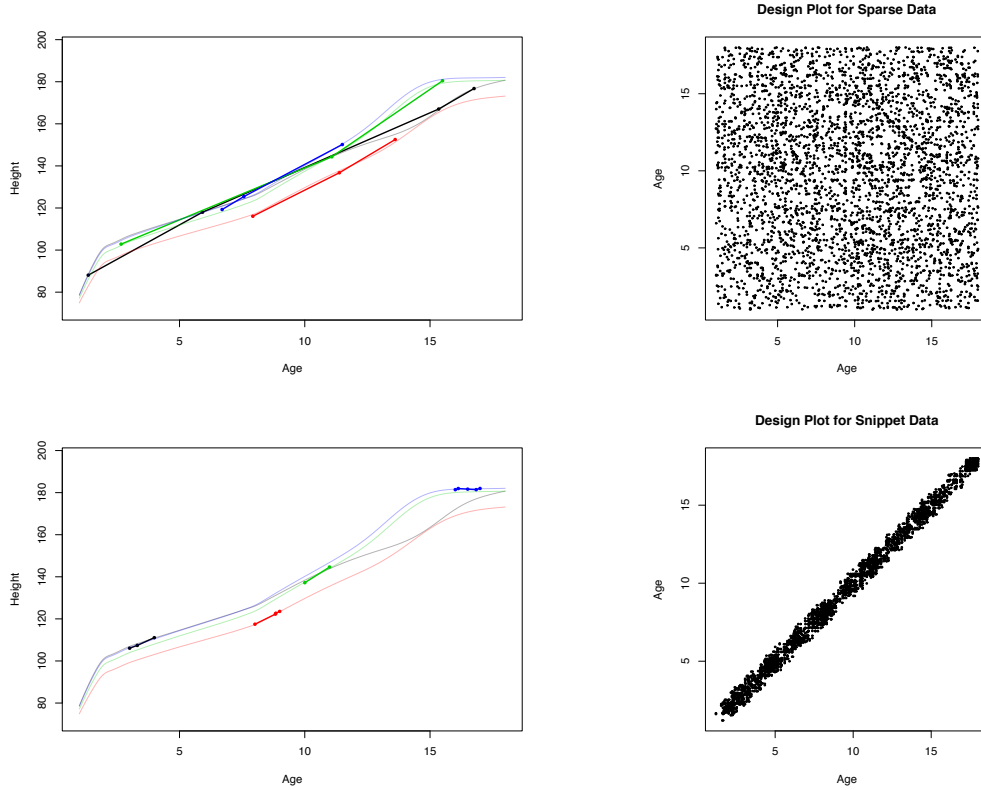


Figure 2: A comparison between sparse longitudinal data and snippet data demonstrating some of the difficulties posed by snippet data. Data were simulated based on the first three functional principal components of Berkeley Growth curves. Design plots are based on 300 sparse or snippet trajectories, respectively.

It is well established in the Alzheimer’s disease (AD) literature that the volume of the hippocampus is decreasing more rapidly for those suffering from Alzheimer’s and dementia than it is under normal aging. The hippocampus is a region in the brain associated with memory, making hippocampal volume an important biomarker in Alzheimer’s diagnosis (Mu and Gage 2011). Therefore, one is interested in modeling the hippocampal volume longitudinally. Here we take the response to be the log hippocampal volume, defined as the log of the sum of the hippocampal lobe volumes (left and right).

An unfortunate aspect of AD is that it can only be diagnosed post-mortem. As

such, there is no way of knowing which patients have AD; we can only gain insight via cognitive tests. The subjects in this study have been classified in a clinical evaluation as having normal cognitive function, mild cognitive impairment (MCI), or dementia based on the SENAS (Spanish and English Neuropsychological Assessment Scales) cognitive test (Mungas et al. 2004). Information regarding the different clinical classifications may be found in Albert et al. (2011); McKhann et al. (2011); Sperling et al. (2011).

Figure 3 displays some important features of the dataset. The snippet characteristics are apparent. With an age range spanning roughly 42 years, the average range of observations per subject averages only 4.2 years. While there seem to be differences between the normal and impaired groups, one has difficulty describing these differences in terms of mean decline as the data form a cloud with no clear patterns. In particular, it is not entirely obvious whether there is an overall decrease over time. We claim that in fact, there is a clear difference between groups and that the rate of hippocampal atrophy is more dramatic than Figure 3 implies.

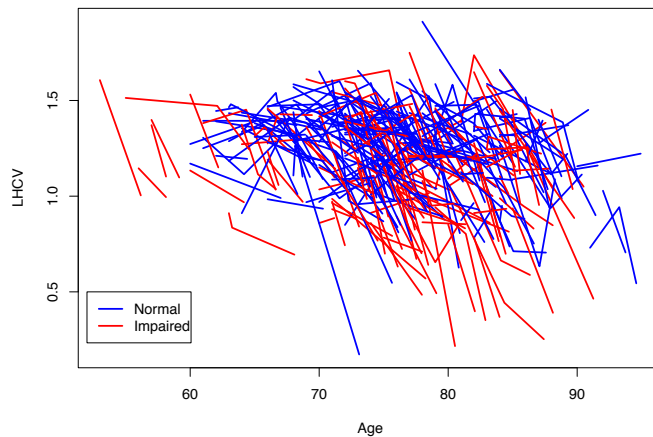


Figure 3: Log hippocampal volumes (LHCV) for all subjects with multiple measurements, colored by cognitive status: normal subjects are blue, those with at least one MCI or demented cognitive score are shown in red.

It should be noted that there are several subjects with different cognitive classifications over time. For simplification, we define the impaired subjects as those with at least one MCI or demented classification and the normal group as having no MCI nor demented ratings. The difference between the normal and impaired groups, for example, is pronounced in Figure 4 where the groups are plotted separately. While the rates of decline are almost uniformly more severe for the demented group, there seems to be little difference in the mean trend over time with respect to age. Exploratory analysis shows that neither level nor local slope, calculated using a least squares fit on each subjects' measurements, change significantly over chronological age for the demented group. We conclude that chronological age is not informative.

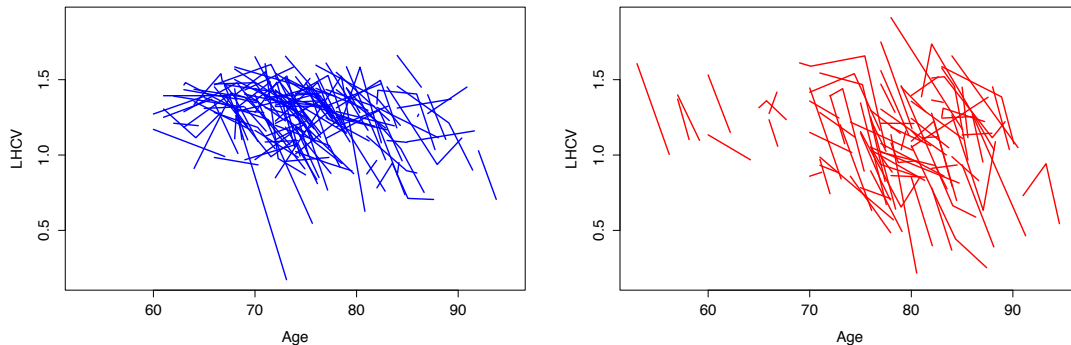


Figure 4: LHCv longitudinal measurements for normal and demented cognitive groups showing a notable difference between groups.

The unavailability of a meaningful absolute time measurement is not unique to AD studies. For instance one may be interested in the growth patterns of tumors. Here the time of interest would not be age, but rather the typically unknown time that has passed since the inception of the tumor. In more complete data, one could register the curves based on some landmark features. With our limited data, however, this is not feasible. We conclude that age is an uninformative time scale, particularly for impaired subjects, and with little information available to register the data, we seek new methodology to

bypass modeling with time directly.

In the case of monotonic processes, Abramson and Müller (1994) found that one can still obtain trajectory information over time as long as information about local level and slope is known for each subject. Furthermore, Abramson and Müller suggest that data in this form can be viewed as bivariate observations of level and slope at some random, unobserved time. Formally, we may write $X_i = f(T_i)$ and $Z_i = f'(T_i) + \epsilon_i$, for $i = 1, \dots, n$, with i.i.d. noise ϵ_i satisfying $E(\epsilon) = 0$ and $E(\epsilon^2) = \sigma^2 < \infty$, where f is a fixed, strictly monotonic function and one observes (X_i, Z_i) . The idea is that for a monotonic function, there exists a function g that relates the slope to the level: $f'(t) = g(f(t))$, where $g(x) = E(Z|X = x)$ and we can use the data to estimate this function using scatterplot smoothers (Fan and Gijbels (1996)). Vittinghoff et al. (1994) proposed a similar model which also relates the slope to level through a differential equation. This approach reflects that due to the short time span of snippet data, the available data do not carry information beyond local level and slope. To extract this local information, one can apply a simple linear least squares fit to the data in each snippet and extract slope and mean estimates.

A key assumption in Abramson and Müller (1994); Vittinghoff et al. (1994) was that one observes noisy measurements from a fixed function f . This targeted an overall mean function, while individual dynamics are of paramount interest, for example in accelerated longitudinal studies. Therefore we extend these methods by allowing observations to come from realizations of a stochastic process, and aim to estimate functionals of the conditional distribution of slopes for a given level, rather than only the mean function.

The organization of this paper is as follows. In Section 2 we introduce the proposed dynamic model, while Section 3 covers estimation procedures. Our main theoretical results are discussed in Section 4. Simulations and an AD application are discussed in Sections 5 and 6, respectively.

2. DYNAMIC MODELING OF THE DISTRIBUTION OF DECLINE RATES

2.1. Basic Model

Assume that Y is a stochastic process that is $k+1$ -times continuously differentiable for $k \geq 1$, defined on some domain \mathcal{T}_0 and let \mathcal{J} be the range of Y restricted to \mathcal{T}_0 . Measurements are generated by observing $Y_i(T_i)$ and $Y'_i(T_i)$ at some random and potentially unobserved subject-specific time T_i , where T is independent of Y . Denote these observations as $X_i := Y_i(T_i)$ and $Z_i := Y'_i(T_i)$ for $i = 1, \dots, n$. Further assume that $T_i \sim f_T$ for some density f_T on \mathcal{T}_0 , and that (X_i, Z_i, T_i) have a joint distribution and are independent of (X_j, Z_j, T_j) for $i \neq j$. A core feature of our model is that the conditional distribution of the slope given the level does not depend on T , which means that the distribution of the rate of decline depends only on the current level but not on the random time where the observation of level and slope takes place. That is,

$$F(z|x) = P(Y'(T) \leq z \mid T, Y(T)) = P(Z \leq z \mid X = x), \quad (1)$$

so that $F(z|x)$ does not explicitly depend on T , which implies that the process is completely determined by the relationship between level and slope. This assumption is similar to assumptions made in Abramson and Müller (1994) and Vittinghoff et al. (1994), where the focus was on estimation of the mean, rather than the conditional distribution. While we focus on the scenario where the conditional distribution $F(z|x)$ does not depend on T , in Section 3, we describe how one can allow for dependence on the observation time T for situations where T is available.

Rather than only aiming at the conditional mean, our goal is to target the distribution of slopes at a given level which then will provide insights into the dynamics of the process. Ultimately we target the conditional quantile trajectories of the process $Y(t)$, which describe the probabilistic time dynamics of the process Y given a starting point

and provide a more comprehensive reflection of the underlying dynamics than the conditional expected trajectories alone. The assumption that the measurements are taken from realizations of a general stochastic process leads to increased flexibility in modeling and accounts for subject-specific variation.

Further examining the nature of (1), simple calculations show that smooth monotonic functions with random components satisfy the assumptions. For a specific example, consider the model $Y(t) = af(bt + c) + d$ where $f(\cdot)$ is a fixed monotone function, and (a, b, c, d) is a random vector with some joint distribution. Examining the conditional probabilistic behavior of this process at a randomly and independently selected time T , and again using the notation $X = Y(T)$, we find

$$\begin{aligned} F(z|x) &= P(Y'(T) \leq z \mid T, Y(T)) \\ &= P(abf'(bT + c) \leq z \mid T, Y(T)) \\ &= P\left(abf'\left(f^{-1}\left(\frac{1}{a}Y(T) - \frac{d}{a}\right)\right) \leq z \mid T, Y(T)\right) \\ &= P\left(abf'\left(f^{-1}\left(\frac{1}{a}X - \frac{d}{a}\right)\right) \leq z \mid X = x\right), \end{aligned}$$

so that $F(z|x)$ is seen not to depend on T whence the model assumptions are satisfied.

Note that in this example, $F(z|x)$ depends on the random quantities (a, b, c, d) and the fixed function f . However, the key observation is that the distribution of slopes at some random time T only depends on the level at that same time T . Therefore we can obtain inference for conditional probabilities involving $Y'(T)$ without explicitly observing T , taking advantage of the monotonicity of the process Y .

2.2. Evolution of Conditional Distributions and Quantiles

Acquiring an estimate of (1) will provide insight into the instantaneous probabilistic dynamics of a process. This conditional distribution tells us where subjects generally are

headed in the immediate future, based on their starting level, not only in the mean but also including the distribution of their slopes of decline. One can readily compute other functionals from this conditional distribution, for example quantiles. In data applications it is additionally of interest to infer how the process behaves over a longer period of time, continuing after time T . To assess long term behavior of the decline process after a random starting time T , we introduce the notion of an α -quantile trajectory, for a given $0 < \alpha < 1$. We first define the *instantaneous α -quantile* at a given level x as $\xi_\alpha(x)$,

$$\xi_\alpha(x) = F^{-1}(\alpha|x), \quad (2)$$

where $F(z|x)$ is defined as in (1).

The function ξ_α describes the α -quantile of slope for a given level, providing information about the instantaneous rate of decline. A simple, yet useful way to utilize $\xi_\alpha(x)$ is to define a class of trajectories that at all times follow the α -quantile of slope given the current level, thus representing a constant quantile of degradation, for example median degradation. Accordingly, given $0 < \alpha < 1$, we define a trajectory $z_{\alpha,x}$ as the solution to an autonomous differential equation

$$\frac{dz_{\alpha,x}(T+s)}{ds} = \xi_\alpha(z_{\alpha,x}(T+s)), \quad (3)$$

with initial condition $z_{\alpha,x}(T+0) = x$. We then refer to the solution function $z_{\alpha,x}(T+\cdot)$ as the *α -quantile trajectory* and note that it depends only on x and α but does not depend on the random time T .

Note that ξ_α is the gradient function relating the slope to the level. Defining quantile trajectories in this way sidesteps T , which is unknown. This approach can be contrasted with the previous strategy (Abramson and Müller 1994; Vittinghoff et al. 1994) for esti-

imating the conditional mean function $\mu_x(T + s)$, which is the function satisfying

$$\frac{d\mu_x(T + s)}{ds} = E(Y'(T + s) \mid Y(T) = \mu_x(T + s)), \quad (4)$$

with initial condition $\mu_x(T + 0) = x$. It is straightforward to estimate the α -quantile trajectories iteratively, using simple numerical integration techniques, such as Euler's method, to solve the defining autonomous differential equation (3).

An alternative way of characterizing the distribution of the process would be to target cross-sectional quantiles. That is, define G_t as the function

$$G_s(y|x) = P(Y(T + s) \leq y \mid Y(T) = x), \quad (5)$$

the distribution of $Y(T + s)$ for a given starting value. Taking the α -quantile for all $s \in \mathcal{T}$ gives the *cross-sectional α -quantile trajectory*

$$q_{\alpha,x}(T + s) = G_s^{-1}(\alpha|x). \quad (6)$$

The cross-sectional quantile $q_{\alpha,x}$ thus explicitly depends on $Y(T+s)$, which is not observed. In general $z_{\alpha,x}$ and $q_{\alpha,x}$ will not be the same, due to basic differences in their definitions. However, according to Proposition 1 below, in many cases $z_{\alpha,x}$ and $q_{\alpha,x}$ will coincide. For this we will require some smoothness and uniqueness assumptions, where C^{k+1} is the space of $k + 1$ -times continuously differentiable functions for $k \geq 1$,

(A1) The cross-sectional quantile trajectories $q_{\alpha,x}$ satisfy $q_{\alpha,x} \in C^{k+1}(\mathcal{T})$ and are monotone in s .

(A2) The cross-sectional quantiles are unique: $G_s(y) = P(Y(T + s) \leq y \mid Y(T) = x)$ is strictly monotone in y for all $s \in \mathcal{T}$.

Assumption (A1) is necessary to ensure that the trajectory $q_{\alpha,x}$ can be written as the solution to an autonomous differential equation, and implies that there exists a function $h \in C^k(\mathcal{J})$, where \mathcal{J} is the range of Y restricted to \mathcal{T} , so that $q_{\alpha,x}$ is the solution to an autonomous differential equation

$$\frac{dq_{\alpha,x}(T+s)}{ds} = h(q_{\alpha,x}(T+s)).$$

The second assumption (A2) guarantees uniqueness of the cross-sectional quantiles so that $q_{\alpha,x}$ is defined uniquely.

Proposition 1. *If the process Y satisfies (A1) and (A2), then α -quantile cross-sectional trajectories and α -quantile trajectories coincide, i.e., $q_{\alpha,x}(T+s) = z_{\alpha,x}(T+s)$ for all $s \in \mathcal{T}$.*

The implication is that under these smoothness and autonomous assumptions we may target $z_{\alpha,x}$ and interpret it as a cross-sectional quantile. This allows us to investigate the conditional median, best and/or worst case scenarios, and all intermediate quantiles, as we will demonstrate in the simulations in section 5 and in the data examples in section 6.

3. ESTIMATION

3.1. Estimation of Conditional Distributions and Quantiles

The task of estimating $z_{\alpha,x}$ can be decomposed into three steps. First, we estimate the conditional distribution $F(z|x)$. Next we use this estimate to obtain an estimate of the instantaneous conditional quantile function ξ_α , according to (2). Finally, this estimate of ξ_α is employed as gradient function in an autonomous differential equation as per (3), and then this equation is solved numerically. The details are as follows.

The data in our application is of the form (X_i, Z_i) for $i = 1, \dots, n$, where the snippet data are generated as follows. First, for the i th subject, a random mechanism selects the underlying trajectory Y_i . Subjects are measured in a window situated around random

times T_i and observations are generated by a second independent random mechanism as $Y_{ij} = Y_i(T_{ij}) + e_{ij}$, for $T_{ij} \in [T_i - \Delta, T_i + \Delta] \subset \mathcal{T}_0$, where e_{ij} are independent measurement errors; an illustration of this is in Figure 1.

For subject i with n_i measurements Y_{ij} at times T_{ij} , $j = 1, \dots, n_i$, one may use the empirical estimators $X_i = \frac{1}{n_i} \sum Y_{ij}$ and $Z_i = \hat{\beta}_{1i}$, where $(\hat{\beta}_{0i}, \hat{\beta}_{1i}) = \operatorname{argmin}_{(\beta_{0i}, \beta_{1i})} \sum_{j=1}^{n_i} (Y_{ij} - \beta_{0i} - \beta_{1i}T_{ij})^2$ for level and slope. When observations are assumed to be independent, as in our case, estimation of conditional distribution functions has been widely studied in the literature (Hall et al. 1999; Li and Racine 2008; Roussas 1969; Samanta 1989; Ferraty et al. 2006; Horrigue and Saïd 2011). Here we outline several methods by which one can estimate the conditional distributions $F(z|x)$ defined in (1). We note that if T is known, one could include it as an additional predictor in the estimation of $F(z|x, T)$.

Binomial regression. Writing the conditional distribution function as $F(z|x) = E(1(Z \leq z) \mid X = x)$ and assuming a linear predictor and a link function g , we can model the conditional distribution parametrically as

$$F(z|x) = E(1(Z \leq z) \mid X = x) = g^{-1}(\beta_0 + \beta_1 x + \beta_2 z). \quad (7)$$

Flexibility can be increased by making use of a generalized additive model

$$F(z|x) = E(1(Z \leq z) \mid X = x) = g^{-1}(\alpha_0 + f_1(x) + f_2(z)), \quad (8)$$

where f_1 and f_2 are assumed to be smooth with $\int f_1 = \int f_2 = 0$. These parametric methods are simple but require strong assumptions. For instance, the shape of the c.d.f. is determined by the unknown link function g . On the positive side, dependence on T and additional covariates can be easily accommodated by including these covariates in the linear predictor, making this approach appealing for some applications.

Empirical c.d.f. based on binning. A basic approach for nonparametric estimation

of a conditional distribution involving two continuous variables is to take a small window around the conditioning variable, selecting the data where the conditioning variable falls into the window, and computing the empirical c.d.f. based on these data. I.e., when estimating $P(Z \leq z \mid X = x)$, one can simply take a window $\{x \pm h\}$ and calculate the empirical c.d.f. over Z for all subjects satisfying $X \in \{x \pm h\}$, or

$$\tilde{F}_B(z|x) = \frac{1}{n} \sum_{i=1}^n 1(Z_i \leq z) 1(X_i \in \{x \pm h\}). \quad (9)$$

This can be extended to include additional covariates but this may incur a curse of dimensionality depending on the number of covariates.

Kernel smoothing. A natural extension of binning is kernel smoothing, analagous to extending a histogram to a smooth density function estimate. This leads to estimators

$$\tilde{F}_K(z|x) = \frac{\sum_{i=1}^n 1(Z_i \leq z) K_h(x - X_i)}{\sum_{i=1}^n K_h(x - X_i)}, \quad (10)$$

where $K_h(u) = h^{-1}K(u/h)$ and K is a kernel function, generally chosen as a smooth and symmetric probability density function. This estimator is well understood and is a simple extension of the binning method (9). Several variants of this estimator have been considered (Hall et al. 1999; Li and Racine 2008).

Joint kernel smoothing. Finally, one might prefer an estimator that is differentiable in x as well as z . A smoothed version of (10) is obtained by replacing the indicator function with a smooth distribution function H :

$$\hat{F}_{JK}(z|x) = \frac{\sum_{i=1}^n H_{h_H}(z - Z_i) K_{h_K}(x - X_i)}{\sum_{i=1}^n K_{h_K}(x - X_i)}. \quad (11)$$

Here K_h is as before with bandwidth h_K and $H_{h_H}(u) = H(u/h_H)$ with possibly different bandwidth h_H . For K one commonly uses a probability density function and H is its

corresponding cumulative distribution function: $H(u) = \int_{-\infty}^u K(t)dt$. This type of estimator was studied in Roussas (1969) and Samanta (1989) and has since been extended to include functional predictors in Ferraty et al. (2006) and Horrigue and Saïd (2011). As we will require differentiability of our estimate of $F(z|x)$, we will use estimator (11) in our theoretical results and implementations.

Given an estimator $\tilde{F}(z|x)$ of $F(z|x)$ one can easily construct an estimate of ξ_α ,

$$\tilde{\xi}_\alpha(x) = \inf\{z : \tilde{F}(z|x) \geq \alpha\}, \quad (12)$$

which we will denote by $\hat{\xi}_\alpha(x)$ if it is based on $\tilde{F}(z|x) = \hat{F}_{JK}(z|x)$ in (11). Our method for estimating $z_{\alpha,x}(T+t)$ involves first using $\tilde{\xi}_\alpha(x)$ in (12) as a plug-in estimate for $\xi_\alpha(x)$ in (3), and then solving the resulting differential equation using numerical methods.

3.2. Numerical Integration of the Differential Equation

The final estimation step is using an estimate of ξ_α to produce an estimate of $z_{\alpha,x}$. To estimate the solution of (3) we may use one of several iterative procedures such as Euler's method or the Runge-Kutta method, along with a uniformly consistent quantile estimate. We first discuss a numerical approximation to the solution $z_{\alpha,x}(T+s)$. Then we examine how this quantity can be estimated from the data. For the sake of simplifying notation, in all of the following we assume that $T = 0$, without loss of generality as $z_{\alpha,x}$ does not depend on T . Then our target becomes $z_{\alpha,x}(s)$ for $s \in \mathcal{T} = (0, \tau]$, where now

$$\frac{dz_{\alpha,x}(s)}{ds} = \xi_\alpha(z_{\alpha,x}(s)) \quad (13)$$

with initial condition $z_{\alpha,x}(0) = x$ to guarantee that the α quantile trajectory starts at the stipulated level x , and again with $\xi_\alpha(x)$ as the α -quantile of the distribution of $Y'(T)$ given $Y(T) = x$.

An approximating solution to $z_{\alpha,x}(\cdot)$ is given by $\{s_i, \psi(s_i)\}$, $i = 0, \dots, m$ for some $m \in \mathbb{N}$ where these quantities are found iteratively using the rule

$$\psi(s_0) = x, \quad s_{i+1} = s_i + \delta, \quad \psi(s_{i+1}) = \psi(s_i) + \delta \Phi(\psi(s_i), \delta, \xi_\alpha), \quad (14)$$

where δ is a small time increment. In the case of Euler's method, we have $\Phi(\psi(s_i), \delta, \xi_\alpha) = \xi_\alpha(\psi(s_i))$, while the Runge-Kutta approximation uses

$$\Phi(\psi(s_i), \delta, \xi_\alpha) = \frac{1}{6}(k_1 + 2k_2 + 2k_3 + k_4),$$

where $k_1 = \xi_\alpha(\psi(s_i))$, $k_2 = \xi_\alpha(\psi(s_i) + \delta k_1/2)$, $k_3 = \xi_\alpha(\psi(s_i) + \delta k_2/2)$, $k_4 = \xi_\alpha(\psi(s_i) + \delta k_3/2)$

To understand how the numerical solution $\{s_i, \psi(s_i)\}$ converges, we consider for a pair $(s^*, z_{\alpha,x}(s^*))$

$$\Delta(s^*, z_{\alpha,x}(s^*), \delta, \xi_\alpha) = \begin{cases} [z_{\alpha,x}(s^* - \delta) - z_{\alpha,x}(s^*)]/\delta & \text{if } \delta \neq 0 \\ \xi_\alpha(z_{\alpha,x}(s^*)) & \text{if } \delta = 0. \end{cases}$$

The local discretization error at a point $(s^*, z_{\alpha,x}(s^*))$ is given by

$$LDE(s^*, z_{\alpha,x}(s^*), \delta) = \Delta(s^*, z_{\alpha,x}(s^*), \delta, \xi_\alpha) - \Phi(z_{\alpha,x}(s^*), \delta, \xi_\alpha). \quad (15)$$

Now let $-\infty < a_1 < a_2 < \infty$. The integration procedure defined by Φ is of order q , for $q \geq 1$ and q is an integer, on $[a_1, a_2]$ if $LDE(s, z_{\alpha,x}, \delta) = O(\delta^q)$ for all $s \in [a_1, a_2]$, $z_{\alpha,x} \in \mathbb{R}$ and for all $g \in C_b^q(\text{range } z_{\alpha,x}|[a_1, a_2])$, where $C_b^q[c_1, c_2]$ denotes the real functions which are q times continuously differentiable and bounded q -th derivative on $[c_1, c_2]$, for $-\infty \leq c_1 < c_2 \leq \infty$. It is well known that Euler's method achieves order $q = 1$, while the Runge-Kutta approximation achieves order $q = 4$ (Gragg 1965).

Of course, the function $\xi_\alpha(x)$ is unknown and must be estimated from the data. We plug in an estimate $\tilde{\xi}_\alpha(x)$ into the right hand side of equation (3) and then carry out the numerical integration as described above. This leads to the estimating differential equation

$$\frac{d\tilde{z}_{\alpha,x}(s)}{ds} = \tilde{\xi}_\alpha(\tilde{z}_{\alpha,x}(s)), \quad (16)$$

for $s \in \mathcal{T} = (0, \tau]$, with initial condition $\tilde{z}_{\alpha,x}(0) = x$. Using the numerical integration outlined above in (14) for this differential equation gives the numerical solution $\{s_i, \tilde{\psi}(s_i)\}$. We establish that under regularity conditions, we obtain uniform consistency for $\tilde{\psi}$ as an estimator of $z_{\alpha,x}$ with the corresponding rate depending on the convergence rate of the integration procedure as well as the uniform convergence rate of the estimator $\tilde{\xi}_\alpha(x)$.

4. THEORETICAL RESULTS

Our main result is Theorem 2 on uniform consistency of an arbitrary estimate $\tilde{\psi}$ of $z_{\alpha,x}$, obtained through numerical integration. Theorem 1 provides consistency for the estimator $\hat{F}_{JK}(z|x)$ and the associated estimator $\hat{\xi}_\alpha$. In particular, we show that $\hat{F}_{JK}(z|x)$ satisfies the assumptions of Theorem 2 and therefore leads to a uniformly consistent estimator of $z_{\alpha,x}$. We require the following conditions:

(B1) $\mathcal{J} = \text{range}(Y)|\mathcal{T}_0 = [c_1, c_2]$ and $\mathcal{Z} = \text{range}(Y')|\mathcal{T}_0 = [d_1, d_2]$, where \mathcal{T}_0 is the time interval over which measurements are taken.

(B2) $f_X(x)$, the marginal density of X , and $f_{X,Z}(x, z)$, the joint density of (X, Z) , satisfy

$$0 < m_1 \leq \inf_{x \in \mathcal{J}} f_X(x) < \sup_{x \in \mathcal{J}} f_X(x) \leq M_1 < \infty$$

and

$$0 < m_2 \leq \inf_{x \in \mathcal{J}, z \in \mathcal{Z}} f_{X,Z}(x, z) < \sup_{x \in \mathcal{J}, z \in \mathcal{Z}} f_{X,Z}(x, z) \leq M_2 < \infty$$

for some constants m_1, m_2, M_1, M_2 .

(B3) With $F^{(i,j)}(x, z) = \frac{\partial^{i+j} F(x, z)}{\partial x^i \partial z^j}$, where $F(x, z)$ is the two-dimensional c.d.f. of (X, Z) , assume that $F^{(i+p, j+p)}(x, z)$ exists and is bounded for $(i, j) = (1, 0), (1, 1), (2, 0)$. Also assume that $f_X(x)$ is $p + 1$ times continuously differentiable.

(B4) The conditional quantiles are unique, i.e. $F(z|x)$ is a strictly monotone function of z in a neighborhood of $\xi_\alpha(x)$.

(B5) $H'(u) = K(u)$ and K is a symmetric, compactly supported kernel which is p -times continuously differentiable, of bounded variation, and satisfies $\int uK(u)du = 0$ and $\int u^2K(u)du < \infty$.

(B6) The bandwidth $h_K = h_H = h_n$ satisfies (i) $\frac{\log n}{nh_n^2} \rightarrow 0$ as $n \rightarrow \infty$, (ii) $h_n = o((\frac{\log n}{n})^{1/4})$, and (iii) The series $\sum_{n=1}^{\infty} \exp\{-\kappa nh_n^4\}$ is convergent for all $\kappa > 0$.

Assumptions (B1) - (B3) are standard assumptions regarding the smoothness and boundedness of the distributions when applying smoothing (Ferraty et al. 2006; Hansen 2008; Samanta 1989). Assumption (B4) guarantees that the target quantiles are unique by stipulating that the conditional c.d.f. must not be flat near the α quantile. Finally, assumptions (B5) and (B6) are typical assumptions for kernel estimators.

Theorem 1. *Under conditions (B1) - (B6), we have that the estimator $\hat{\xi}_\alpha$, defined at (12) and obtained by inverting $\hat{F}_{JK}(z|x)$ in (11) satisfies*

$$\sup_{x \in \mathcal{J}} |\hat{\xi}_\alpha(x) - \xi_\alpha(x)| = O_p \left(h_n + \sqrt{\frac{\log n}{nh_n}} \right) \quad (17)$$

and

$$\sup_{x \in \mathcal{J}} |\hat{\xi}'_\alpha(x) - \xi'_\alpha(x)| = o_p(1). \quad (18)$$

For the proof of Theorem 1, one shows first that the estimator $\hat{F}_{JK}(z|x)$ is well-behaved, whence the estimated driving function $\hat{\xi}_\alpha$ of the autonomous differential equation

in (16) and its derivative are seen to be consistent.

For the following main result, some additional conditions are needed:

(C1) Assume that one has a continuously differentiable function $\tilde{\xi}_\alpha$ satisfying

$$\sup_{x \in \mathcal{J}} |\tilde{\xi}_\alpha(x) - \xi_\alpha(x)| = O_p(\beta_n), \quad \sup_{x \in \mathcal{J}} |\tilde{\xi}'_\alpha(x) - \xi'_\alpha(x)| = o_p(1)$$

for a sequence β_n with $\beta_n \rightarrow 0$, $n\beta_n \rightarrow \infty$ as $n \rightarrow \infty$.

(C2) The function $\Phi(y, \delta, \tilde{\xi}_\alpha)$ defining the numerical integration method (14) is continuous in its first two arguments on $G = \{(y, \delta, \tilde{\xi}_\alpha) : |z_{\alpha,x}(s) - y| \leq \gamma, 0 \leq s \leq \tau, \delta \leq \delta_0\}$ for some given $\gamma > 0$, $\delta_0 > 0$ and satisfies $|\Phi(y_1, \delta, \tilde{\xi}_\alpha) - \Phi(y_2, \delta, \tilde{\xi}_\alpha)| \leq L|\tilde{\xi}_\alpha(y_1) - \tilde{\xi}_\alpha(y_2)|$ for some $L > 0$ and for all $y_1, y_2, \delta \in G$.

(C3) The integration method is of order q , i.e., the local discretization error satisfies

$$|LDE(s, y, \delta)| = |\Delta(s, y, \delta, \tilde{\xi}_\alpha) - \Phi(y, \delta, \tilde{\xi}_\alpha)| = O(\delta^q)$$

for $s \in \mathcal{T}$, $\delta \leq \delta_0$, $y = z_{\alpha,x}(s)$.

Assumption (C1) is satisfied under the conditions of Theorem 1 and ensures consistency of the gradient function estimate which drives estimation; the condition on the derivative is needed to control the remainder in the local estimation error. Assumptions (C2) - (C3) deal with the smoothness and convergence of the numerical integration procedure. We note that both the Euler and Runge-Kutta methods satisfy these requirements.

Theorem 2. *For an estimator $\tilde{\xi}_\alpha$ of ξ_α which satisfies (C1) and an integration procedure which satisfies (C2), (C3), we have that the numerical solution $\tilde{\psi}$ of the initial value problem (16) satisfies*

$$\sup_{s \in \mathcal{T}} |\tilde{\psi}(s) - z_{\alpha,x}(s)| = O(\delta_n^q) + O_p(\beta_n), \quad (19)$$

where $\delta_n = |\mathcal{T}|/n$ is the step size used in the integration procedure and $|\mathcal{T}| = \tau$ is the length of the interval \mathcal{T} .

Theorems 1 and 2 imply that under regularity conditions, one can estimate $z_{\alpha,x}$ using the joint kernel described in (11) setting $\tilde{\xi} = \hat{\xi}$ and a well-behaved numerical integration procedure to obtain a uniform convergence rate of $O(\delta_n^q) + O_p(h_n + \sqrt{\frac{\log n}{nh_n}})$.

5. FINITE SAMPLE PERFORMANCE

5.1. Simulation Study

To evaluate the performance of our method, we simulate snippet data from two simulated processes. The first is exponential in nature, generated from sample curves following $Y(t) = \exp\{-b(t+1)\}$ where b is a $\mathcal{U}(.3, .5)$ random variable. The second is a quadratic process, using $Y(t) = a - bt^2$, where $a \sim \mathcal{U}(190, 200)$, $b \sim \mathcal{U}(.2, .8)$ and a is independent of b . In both scenarios the time domain is the interval $(0, 10)$. Plots of artificial one-year snippets generated from these curves are shown in Figure 5.

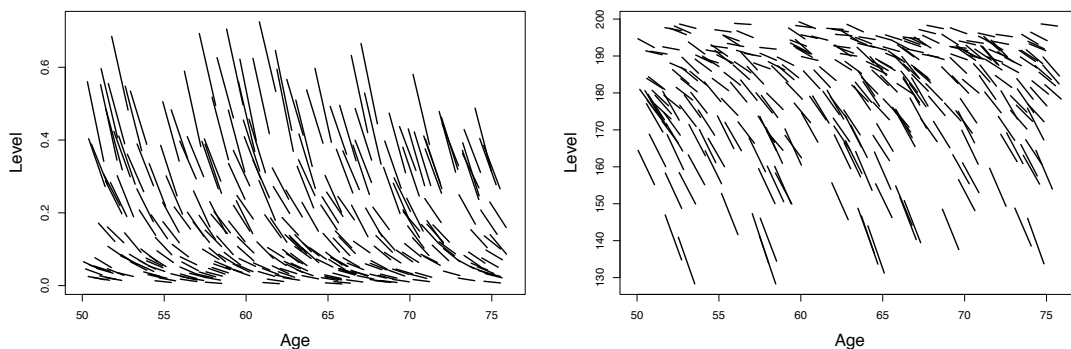


Figure 5: Generated curves and snippets with randomly assigned ages from the exponential (left) and quadratic (right) simulations.

The simulations are chosen to mimic natural occurring phenomena. For example, the quadratic decline process describes a situation where decline is amplified as time increases. In both simulations, we sample $X_i = (Y_i(T_i) + Y_i(T_i+1))/2$ and $Z_i = (Y_i(T_i+1) - Y_i(T_i))/1$

with the T_i having a $\mathcal{U}(0, 9)$ distribution. While the underlying processes are highly nonlinear, our observations only carry local linear information. Importantly, our method allows us to pool information from all subjects to uncover the true nonlinear relationship without using any parametric assumptions.

Our simulation study examines the effect of the estimation procedure, sample size, and choice of α . The estimation procedures considered are: the binomial regression model in (7) using a logistic link, the kernel estimator in (10) with bandwidth .01 in the exponential case and 1 in the quadratic case and Gaussian kernel, and the joint kernel estimator in (11) with $h_K = .01$ and $h_H = .001$ in the exponential case and $h_K = 1$ and $h_H = .05$ in the quadratic case and Gaussian kernel. We vary the sample size using $n = 300$ and 1000. The probability α is varied over $\alpha = \{.05, .25, .5, .75, .95\}$.

As a measure of quality we consider the average integrated squared error (AISE) when repeating the simulations $N = 100$ times. For our target $z_{\alpha,x}(s)$ for $s \in (0, \tau]$ and its estimator, the AISE is defined as

$$\text{AISE} = \frac{1}{100} \sum_{i=1}^{100} \int_0^{\tau} (z_{\alpha,x}(s) - \tilde{\psi}^{(i)}(s))^2 ds,$$

where $\tilde{\psi}^{(i)}(s)$ is the functional estimate of $z_{\alpha,x}(s)$ in the i^{th} repetition. The time domain in the exponential case is chosen to be $(0, 8]$ since after time $s = 8$ many of the trajectories are flat, while in the quadratic case the chosen time domain is $(0, 5]$. We find that the kernel type estimators outperform the logistic regression model, owing to the fact that the parametric model lacks flexibility. As shown in Figure 6 our methods perform quite well, even with a modest sample size of 300.

Not surprisingly, Figure 6 demonstrates that the extreme quantile trajectories are more difficult to estimate, accounting for the larger spread toward the end of the time domain. The more moderate quantiles, such as the median, however, are estimated quite

accurately.

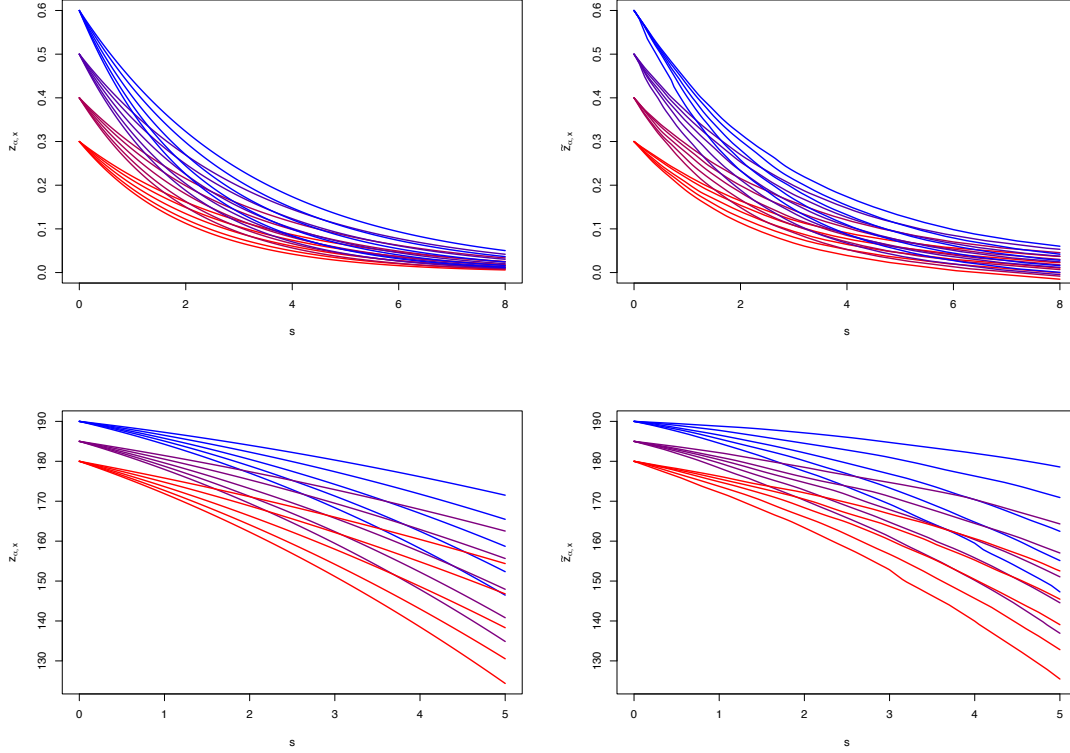


Figure 6: Results of single simulations for various starting levels, and $\alpha \in \{.05, .25, .5, .75, .95\}$ for the exponential (top) and quadratic (bottom) cases. The left panels show the true $z_{\alpha,x}$ while the right panels show our estimate based on a kernel estimate of $F(z|x)$, with a sample size of 300. For clarity, curves starting from different levels are colored differently.

The results for the exponential simulation study in Table 1 reveal that the kernel estimators described in (10) and (11) outperform the logistic method in all cases. In the case of small sample sizes the kernel estimator (10) performs slightly better than the joint kernel estimator (11). Median trajectories are estimated quite accurately in all scenarios in the exponential simulation. The corresponding results for the quadratic simulation are in Table 2 in the Supplement, where again the nonparametric methods is seen to outperform the logistic model.

Sample Size	α	Logistic Model	Kernel Smoothing	Joint Kernel
300	.05	6.30	.447	.425
	.25	.508	.092	.109
	.50	.184	.123	.161
	.75	.845	.108	.121
	.95	5.99	.246	.252
1000	.05	6.33	.456	.456
	.25	.491	.054	.048
	.50	.155	.106	.105
	.75	.810	.110	.111
	.95	5.88	.284	.280

Table 1: AISE scores ($\times 1000$) for various scenarios in the exponential simulation, each with a starting value of $x = 0.4$.

5.2. Simulating Snippets from the Berkeley Growth Data

We also investigate the performance of our methods using growth curves from the Berkeley Growth Study. The Berkeley Growth dataset contains dense growth curves for 39 boys, with measurements spanning ages one to eighteen. To enlarge our sample size, we generate synthetic growth curves by first estimating the mean function as well as the first three eigenfunctions and functional principal component scores for each subject; the first three components accounted for 95% of the variability in the original data. We then resample from the distribution of principal component scores and use these scores to reconstruct a sample of 300 growth curves.

Given these synthetic growth curves, we create artificial snippets by randomly selecting two measurements, one year apart, for each subject, which are displayed in the left panel of Figure 7; the right panel shows a scatterplot of (X_i, Z_i) , along with the gradient functions $\hat{\xi}_\alpha(x)$ estimated from the conditional distribution estimate $\hat{F}_{JK}(z|x)$. Given the level/slope pairs (X_i, Z_i) , our goal is to estimate the conditional quantile trajectories $z_{\alpha,x}(s)$ for $s \in (0, 10]$, $\alpha \in \{.10, .25, .50, .75, .90\}$, where we condition on the starting level $X = 120$. We can easily assess how the estimated α quantile trajectories relate to the sample of actual simulated trajectories by enforcing that each of the functional observations

pass through the point $(0, 120)$; see Figure 8.

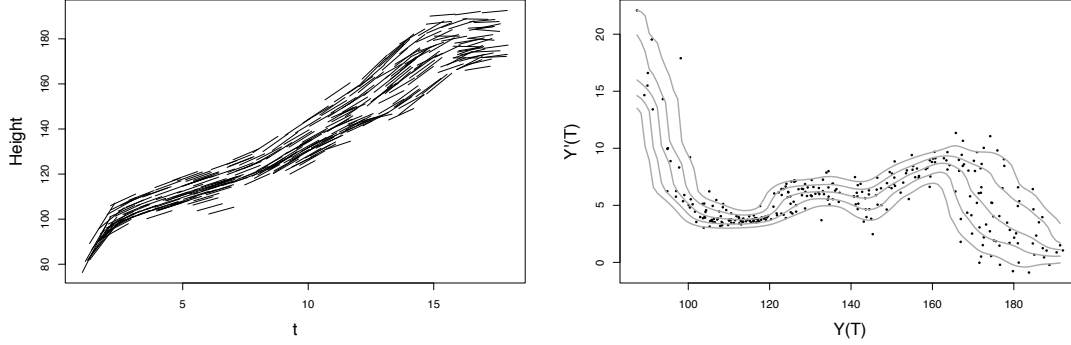


Figure 7: Artificial snippets created from the Berkeley Growth data (left) and corresponding estimates of $\xi_\alpha(x)$ for $\alpha \in \{.10, .25, .50, .75, .90\}$ (right).

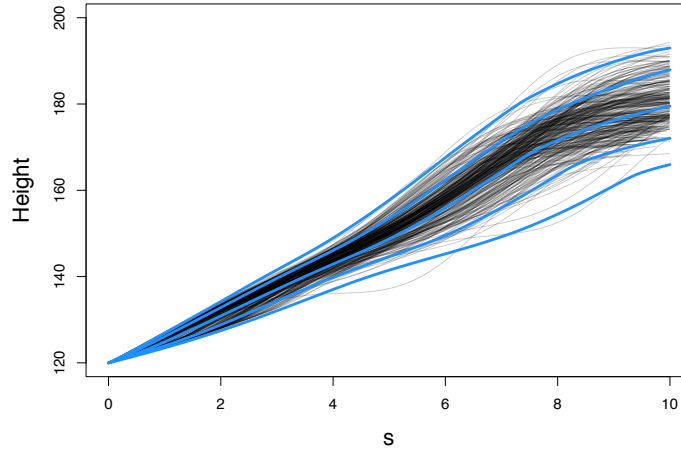


Figure 8: Simulated conditional trajectories (light grey) sharing the same starting level with the estimated conditional quantile trajectories (blue), which are shown for quantile levels $\alpha \in \{.10, .25, .50, .75, .90\}$.

Figure 8 demonstrates that the proposed method reflects nonlinearities in the data quite well given that the available data are very limited. We emphasize that the age at which the subjects entered the study was not used in estimation; the conditional quantile trajectories were solely estimated from the information in levels and slopes (X_i, Z_i) .

6. APPLICATION TO ALZHEIMER'S DATA

We now return to the motivating dataset consisting of hippocampal volume measurements. The dataset of interest contains measurements of longitudinal hippocampal volumes for 270 subjects, with ages ranging from 47 to 96. Demented and MCI subjects are pooled, forming a cognitively impaired group. For these data we estimate the $z_{\alpha,x}$ for varying levels of α , noting that quantiles with steeper declines will not be estimable for the same time duration as those with less severe trajectories. As the kernel estimator performed best in the simulation study, we use it as our estimation method. Our results align with intuition and previous scientific findings. For example, Figure 9 shows that the decline rate is more severe for the demented and MCI groups than it is for the normal group.

Another interesting result is that hippocampus atrophy is accelerating for lower levels, especially among the demented subjects (see Figure 12 in the Supplement). This characteristic implies that the decline of affected subjects is accelerating, which is a confirmation of what has already been documented in Alzheimer's studies (see Sabuncu et al. (2011) in which the authors caution practitioners from ignoring the nonlinear trend in hippocampal atrophy). Figure 9 shows clear differences in distribution for the two groups, demonstrating future potential trajectories in a data driven way and illuminating the differences between cognitive groups.

It is of great interest to assess individuals by comparing them to the overall sample. This is done visually for a small subset of individuals in Figure 10, where we examine each subject's slope relative to the estimated conditional quantile trajectories. The plots in Figure 9 represent estimates of population conditional quantiles and can be used to examine the severity of a given subject's trajectory. For this we estimate $z_{\alpha,x}$ starting from the subject's first observation. A demonstration of this procedure on a representative sample of six individuals (three in each cognitive group) is shown in Figure 10. This approach offers a useful way to evaluate an individual's trajectory, based on pooling

information from the entire sample. For example, one can see that Subject A is on a very severe trajectory with respect to the normal cognitive group. On the other hand Subject F, though cognitively impaired, is only on a mildly declining trajectory relative to the rest of the cognitively impaired group.

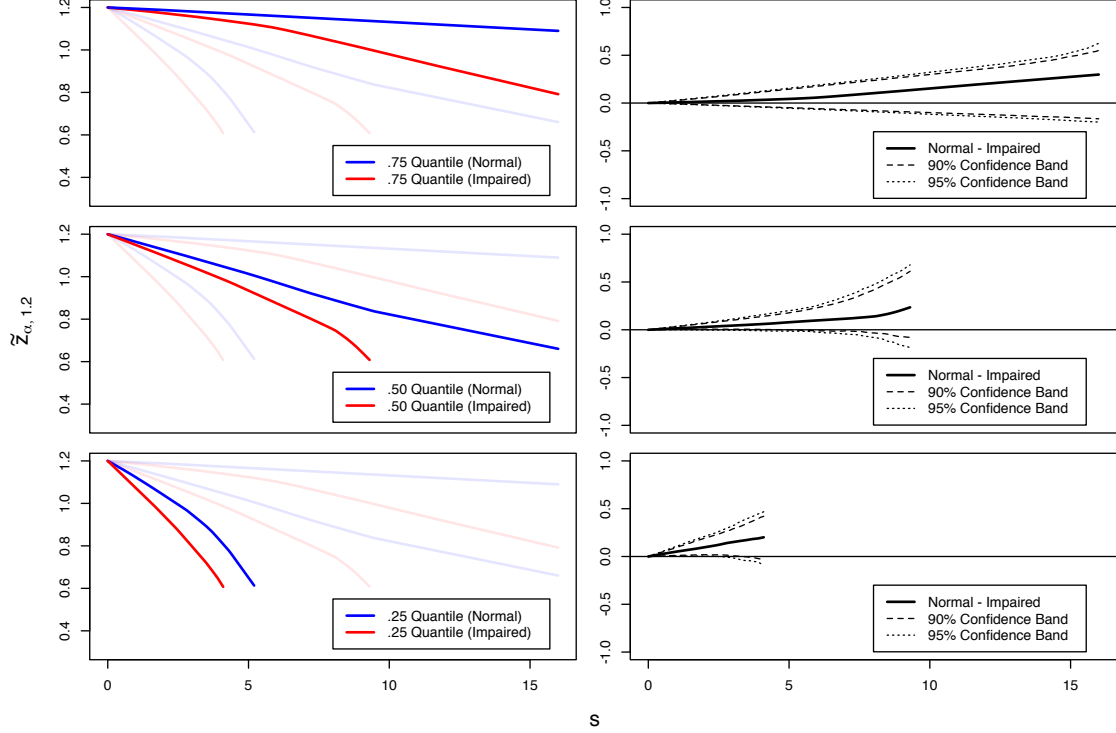


Figure 9: Estimated quantile trajectories conditioned on $x = 1.2$ for normal and MCI/demented groups using the kernel method with bandwidth .12 and Gaussian kernel (left). From top to bottom, α varies over .75, .50, and .25. The right panels show the difference in trajectories between groups, along with 90% and 95% bootstrap confidence bands for the difference

We can take our analysis a step further in making ad hoc predictions about a subject's future trajectories. The idea is to estimate conditional α quantile trajectories $z_{\alpha, x}$ for various α , starting from the subject's last measurement. To ensure that the trajectories align with the subject's snippet, we require that the quantile trajectories do not deviate

too much near the last observation. To achieve this, we first calculate the quantile on which the subject is traveling, and then employ quantile trajectories where $\alpha = \alpha(s)$ depends on the time difference between the prediction and the subject's last observation.

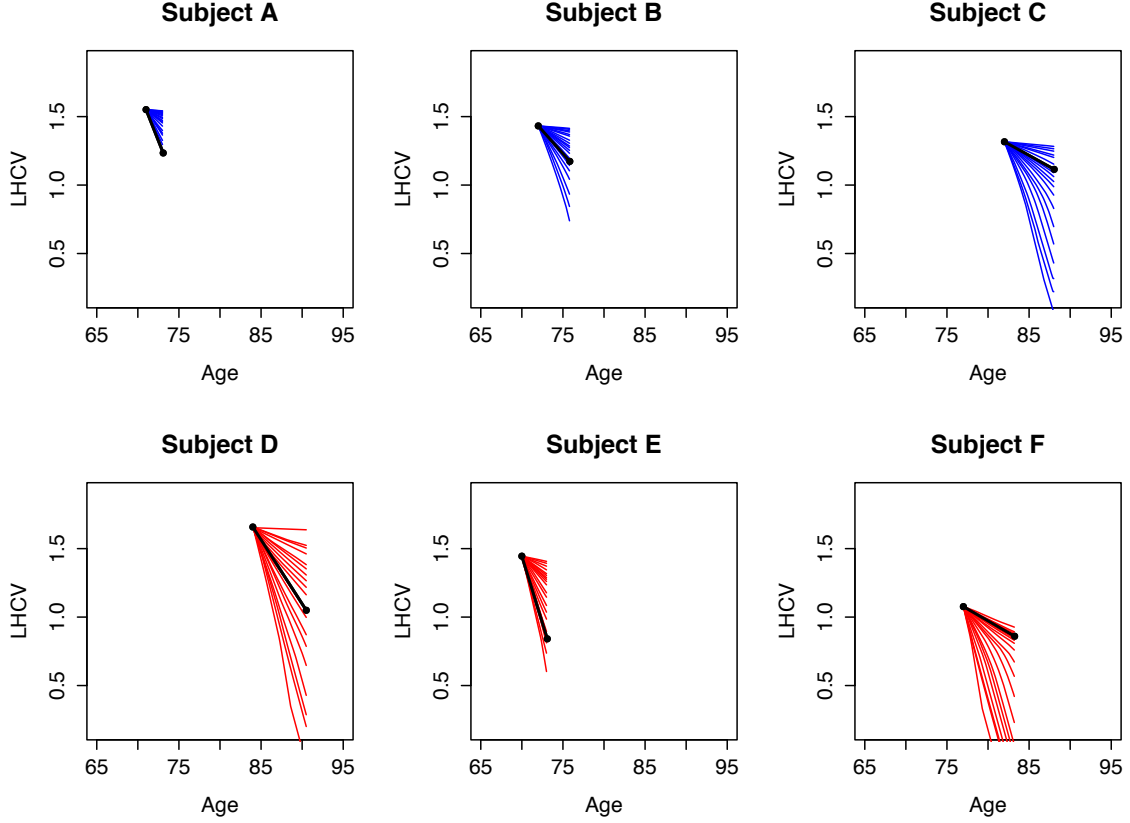


Figure 10: A subset of six individual snippets with corresponding $z_{\alpha,x}$ trajectories originating from the first observation point for each subject. Here, $\alpha \in \{.05, \dots, .95\}$. The black dots are actual observations for each subject; each of these subjects has two observations. The subjects in the top row are from the normal group while the subjects on the bottom row are from the cognitively impaired group.

Specifically, if a subject's snippet is traveling at a given quantile α^* , in estimating the

α quantile trajectory we define

$$\alpha(s) = \begin{cases} \alpha^* + \frac{\alpha - \alpha^*}{S^*} s & \text{if } s < S^* \\ \alpha & \text{if } s \geq S^* \end{cases}, \quad (20)$$

where S^* controls how long the prediction trajectory must adhere to the subject's snippet. In practice, we choose a subject specific $S_i^* = \frac{1}{2}(T_{in_i} - T_{i1})$ to reflect the length of the subject's snippet. We estimate α^* by comparing a subject's slope Z_i to the estimated conditional distribution $\tilde{F}_K(z|y_{i,n_i})$, where y_{i,n_i} is the subject's last observation. An illustration of $\alpha(s)$ can be found in Figure 13 in the Supplement.

In Figure 11, we demonstrate a useful application of these predicted quantile trajectories. For each subject, we estimate the trajectory if a subject were to remain at the same quantile α^* throughout; this curve is shown in black. Additionally, we estimate a range of α quantile trajectories under the constraint that early in the prediction, each α must be close to α^* . After time S_i^* , the α quantile trajectories are unconstrained.

To demonstrate this prediction method, we use the same six individuals as in Figure 10. Prediction in this way is flexible and allows one to pool information from the sample while simultaneously enforcing a degree of compliance with a subject's snippet measurements.

7. DISCUSSION

The problem of longitudinal snippet data is common, especially in accelerated longitudinal medical or social science studies where dense measurements over a long period of time are often not available due to logistical problems. When dealing snippet data one may also face a lack of information about absolute time, which adds to the challenge in assessing the dynamics of the underlying process. We distill the available sparse slope and level information to identify a dynamical system that generates the data and infer information about the random trajectories by introducing the dynamic conditional α quantile

trajectories. Our approach relies on the monotonicity of the underlying processes, which makes it possible to adopt the level of the process as a reference as opposed to time. We demonstrate that the conditional quantile trajectories can be consistently estimated and their estimation, given an initial value, is straightforward.

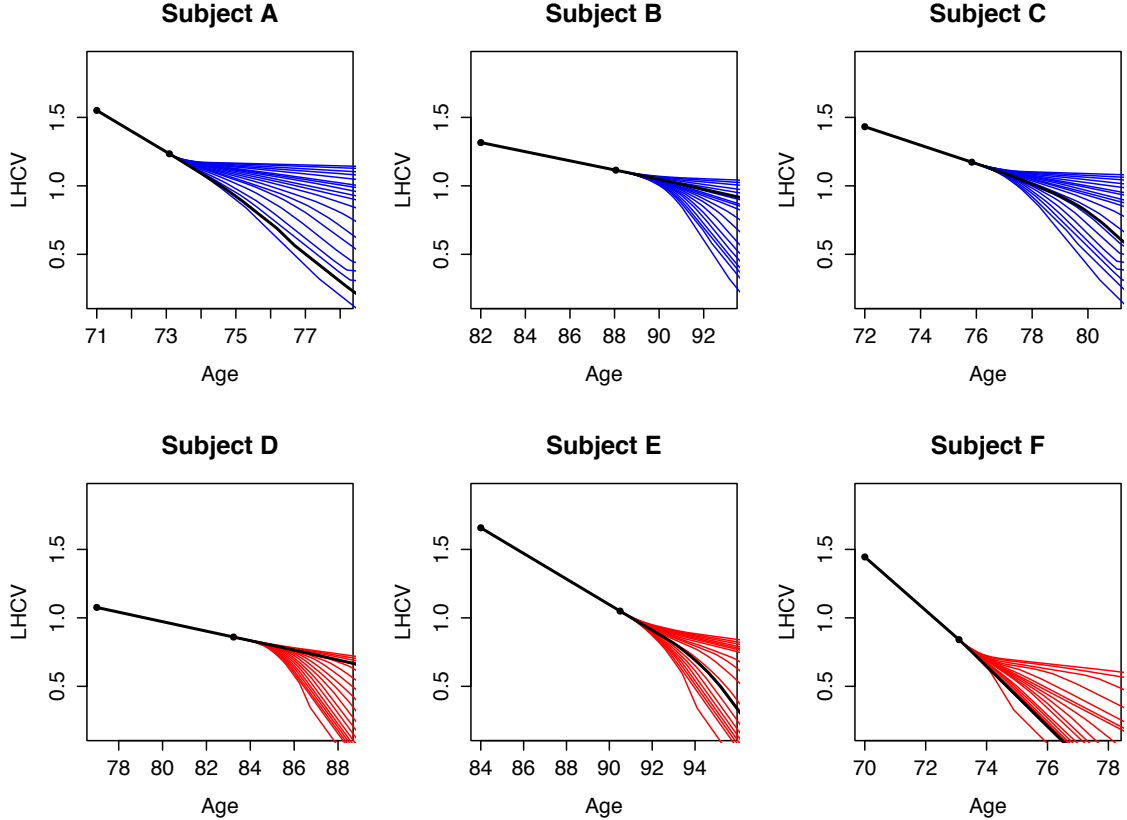


Figure 11: α -quantile prediction trajectories where S^* is chosen to be half the length of timespan of the subject's snippet. The black curves that continue the original observed data snippet which correspond to the linear initial part represent estimated α^* prediction trajectories, where α^* is the estimated quantile of slopes for each subject, conditioned on their last observation. The black dots are the subjects' actual measurements.

While our methods have been motivated by the challenges posed by an Alzheimer's dataset, we note that the proposed dynamic analysis is applicable to degradation studies or accelerated longitudinal studies when underlying processes are monotone. Instead of

examining curves over time, in the monotonic case one can model curves over level. The proposed methods may also prove useful in and can be easily adapted to the case where (absolute) time is actually available. For example, in the logistic models described in (7) and (8) as well as in the nonparametric settings of (10) and (11), age or any other time variable can be easily included in the model as an additional covariate. Our methods and especially the instantaneous α -quantile and the resulting α -quantile trajectory provide useful information about the dynamics of very sparsely observed processes. The proposed estimates perform well and this method will be a useful tool to recover and predict conditional time-dynamic processes in the presence of limited data.

REFERENCES

- Abramson, I. and Müller, H.-G. (1994), “Estimating direction fields in autonomous equation models, with an application to system identification from cross-sectional data,” *Biometrika*, 81, 663–672.
- Albert, M. S., DeKosky S. T., Dickson D., Dubois, B., Feldman, H. H. Feldman, Fox, N. C., Gamst, A., Holtzman, D. M., Jagust, W. J., Petersen, R. C., Snyder, P. J., Carillo, M. C., Thies, B., Phelps, C. H (2011), “The diagnosis of mild cognitive impairment due to Alzheimer’s disease: recommendations from the National Institute on Aging-Alzheimer’s Association workgroups on diagnostic guidelines for Alzheimer’s disease,” *Alzheimer’s & Dementia : The Journal of the Alzheimer’s Association*, 7, 270–279.
- Baskin-Sommers, A.R., Waller, R., Fish, A.M., Hyde, L.W. (2015), “Callous-unemotional traits trajectories interact with earlier conduct problems and executive control to predict violence and substance use among high risk male adolescents,” *Journal of Abnormal Child Psychology*, 43, 1529–1541.
- Brault, M.C., Meuleman, B., Bracke, P. (2011), “Depressive symptoms in the Belgian

- population: disentangling age and cohort effects,” *Social Psychiatry and Psychiatric Epidemiology*, 47, 903–915.
- Brumback, B., Rice, J. (1998), “Smoothing spline models for the analysis of nested and crossed samples of curves,” *Journal of the American Statistical Association*, 93, 961–994.
- Coffey, N., Hinde, J., Holian, E. (2014), “Clustering longitudinal profiles using P-splines and mixed effects models applied to time-course gene expression data,” *Computational Statistics and Data Analysis*, 71, 14–29.
- Delaigle, A. and Hall P. (2013), “Classification using censored functional data,” *Journal of the American Statistical Association*, 108, 1269–1283.
- Fan, J. and Gijbels, I. (1996), *Local polynomial modelling and its applications*, Chapman & Hall/CRC.
- Ferraty, F., Laksaci, A., Vieu, P. (2006), “Estimating some characteristics of the conditional distribution in nonparametric functional models,” *Statistical Inference for Stochastic Processes*, 9, 47–76.
- Ford, K., Hurd, N., Jagers, R., Sellers, R. (2012), “Caregiver experiences of discrimination and African American adolescents’ psychological health over time,” *Child Development*, 84, 485–499.
- Galbraith, S., Bowden, J., Mander, A. (2014), “Accelerated longitudinal designs: An overview of modelling, power, costs and handling missing data,” *Statistical Methods in Medical Research*, 2014, 0962280214547150.
- Galla, B., Wood, J., Tsukayama, E., Har, K., Chiu, A., Langer, D. (2014), “A longitudinal multilevel model analysis of the within-person and between-person effect of effortful engagement and academic self-efficacy on academic performance,” *Journal of School Psychology*, 52, 295–308.
- Gragg, W.B.(1965), “On extrapolation algorithms for ordinary initial value problems,”

- Journal of the Society for Industrial and Applied Mathematics: Series B, Numerical Analysis*, 2, 384–403.
- Guo, W. (2004), “Functional data analysis in longitudinal settings using smoothing splines,” *Statistics in Medical Research*, 13, 49–62.
- Hall, P., Wolff, R. C., Yao, Q. (1999), “Methods for estimating a conditional distribution function,” *Journal of the American Statistical Association*, 94, 154–163.
- Hansen, B. E. (2008) “Uniform convergence rates for kernel estimation with dependent data,” *Econometric Theory*, 24, 726–748.
- Horrigue, W. and Saïd, E. O. (2011), “Strong uniform consistency of a nonparametric estimator of a conditional quantile for censored dependent data and functional regressors,” *Random Operators and Stochastic Equations*, 19, 131–156.
- Jiang, C.-R., Wang, J.-L. (2011), “Functional single index model for longitudinal data,” *The Annals of Statistics*, 39, 362–388.
- Kraus, D. (2015), “Components and completion of partially observed functional data,” *Journal of the Royal Statistical Society: Series B (Statistical Methodology)*, 77, 777–801.
- Liebl, D., Kneip, A. (2016), “On the optimal reconstruction of partially observed functional data,” *Preprint*, http://www.dliebl.com/files/Liebl_Kneip_FDA_Pred_2016.pdf.
- Li, Q. and Racine, J. S. (2008), “Nonparametric estimation of conditional CDF and quantile function with mixed categorical and continuous data,” *Journal of Business and Economic Statistics*, 26, 423–434.
- McKham, G. M., Knopman, D. S., Chertkow, H., Hyman, B. T., Clifford, J., Jack, C.R. Jr., Kawas, C. H., Klunk, W. E., Koroshetz, W. J., Manly, J. J., Mayeux, R., Mohs, R. C., Morris, J. C., Rossor, M. N., Scheltens, P., Carrillo, M. C., Thies, B., Weintraub, S., Phelps, C. H. (2011), “The diagnosis of dementia due to Alzheimer’s disease: recommendations from the National Institute on Aging-Alzheimer’s Association work-

- groups on diagnostic guidelines for Alzheimer’s disease,” *Alzheimer’s & Dementia : the Journal of the Alzheimer’s Association*, 7, 263–269.
- Mu, Y. and Gage, F. (2011) “Adult hippocampal neurogenesis and its role in Alzheimer’s disease,” *Molecular Neurodegeneration*, 6:85.
- Mungas, D., Reed, B., Crane, P., Haan, M., González H. (2004), “Spanish and English Neuropsychological Assessment Scales (SENAS): further development and psychometric characteristics,” *Psychological Assessment*, 16, 347–359.
- Raudenbush, S. and Chan, W.-S. (1992), “Growth Curve Analysis in Accelerated Longitudinal Designs,” *Journal of Research in Crime and Delinquency*, 29, 387–411.
- Rice, J. (2004), “Functional and longitudinal data analysis: Perspectives on smoothing,” *Statistica Sinica*, 631–647.
- Rice, J., Wu, C. (2001), “Nonparametric mixed effects models for unequally sampled noisy curves,” *Biometrics*, 57, 253–259.
- Roussas, G. (1969), “Nonparametric estimation of the transition distribution function of a Markov process” *The Annals of Mathematical Statistics*, 40, 1386–1400.
- Sabuncu, M.R., Desikan, R.S., Sepulcre, J., Yeo, B.T., Liu, H., Schmansky, N.J., Reuter, M., Weiner, M.W., Buckner, R.L., Sperling, R.A., Fischl, B. (2011), “The dynamics of cortical and hippocampal atrophy in Alzheimer’s disease,” *Archives of Neurology*, 68, 1040–1048.
- Samanta, M. (1989), “Non-parametric estimation of conditional quantiles,” *Statistics and Probability Letters*, 7, 407–412.
- Sperling, R. A., Aisen, P. S., Beckett, L. A., Bennett, D. A., Craft, S., Fagan, A. M., Iwatsubo, T., Jack, C. R. Jr., Montine, T. J., Park, D. C., Reiman, E. M., Rowe, C. C., Siemers, E., Stern, Y., Yaffe, K., Carrillo, M. C., Thies, B., Morrison-Bogorad, M., Wagster, M. V., Phelps, C. H. Phelps (2011), “Toward defining the preclinical stages of Alzheimer’s disease: recommendations from the National Institute on Aging-

- Alzheimer's Association workgroups on diagnostic guidelines for Alzheimer's disease," *Alzheimer's & Dementia : The Journal of the Alzheimer's Association*, 7, 280–292, 2011.
- Stanik, C.E., McHale, S.M., Crouter, A.C. (2013), "Gender dynamics predict changes in marital love among African American couples," *Journal of Marriage and Family*, 75, 795–807.
- Staniswalis, J., Lee, J. (1998), "Nonparametric regression analysis of longitudinal data," *Journal of the American Statistical Association*, 93, 1403–1418.
- Vittinghoff, E., Malani, H.M., Jewell, N.P (1994), "Estimating patterns of CD4 lymphocyte decline using data from a prevalent cohort of HIV infected individuals," *Statistics in Medicine*, 13, 1101–1118.
- Wang, N. (2003), "Marginal nonparametric kernel regression accounting for within-subject correlation," *Biometrika*, 90, 43–52.
- Wang, N., Carroll, R.J., and Lin, X. (2005), "Efficient semiparametric marginal estimation for longitudinal/clustered data," *Journal of the American Statistical Association*, 100, 147–157.
- Yao, F., Müller, H.-G., and Wang, J.-L. (2005), "Functional data analysis for sparse longitudinal data," *Journal of the American Statistical Association*, 100, 577–590.

SUPPLEMENT: PROOFS

Proof of Proposition 1: At $s = 0$ the conditional quantile must be equal to x , i.e.,

$$q_{\alpha,x}(T+0) = x.$$

This must be the case since the conditional quantile is based on a starting value of $Y(T) = x$. Next, since $q_{\alpha,x}$ is smooth, it must hold that

$$\frac{dq_{\alpha,x}(T+0)}{dt} = \xi_{\alpha}(x),$$

i.e., the slope of the cross-sectional quantile trajectory at $s = 0$ must equal the α -quantile of slopes at $s = 0$. From these two facts we have that the slope field that describes the behavior of $q_{\alpha,x}$ at $s = 0$ is made up of conditional α -quantiles of slopes, since we can condition on any level $x \in \mathcal{J}$. Now since the differential equation is autonomous, the starting time is arbitrary so for all $s \in \mathcal{T}$, and for all possible starting levels x , we have that the conditional cross-sectional quantile must travel on the conditional α -quantile of slopes. This behavior precisely defines the α -ICQ $z_{\alpha,x}$.

Proof of Theorem 1: Equation (17) is a direct consequence of theorems in Ferraty et al. (2006) and Horrigue and Saïd (2011).

For (18), by the Implicit Function Theorem, we have

$$\xi'_{\alpha}(x) = -\frac{\partial F(z|x)}{\partial x} \times \left(\frac{\partial F(z|x)}{\partial z} \right)^{-1} \Big|_{z=\xi_{\alpha}(x)}$$

and

$$\tilde{\xi}'_{\alpha}(x) = -\frac{\partial \tilde{F}_{JK}(z|x)}{\partial x} \times \left(\frac{\partial \tilde{F}_{JK}(z|x)}{\partial z} \right)^{-1} \Big|_{z=\tilde{\xi}_{\alpha}(x)}.$$

Using the convention that $F^{(i,j)}(x, z) = \frac{\partial F(x, z)}{\partial x^i \partial z^j}$ where $F(x, z)$ is the two-dimensional

c.d.f. of (X, Z) , this leads to

$$\begin{aligned}\xi'_\alpha(x) &= \frac{f'_X(x)F^{(1,0)}(x, z) - f_X(x)F^{(2,0)}(x, z)}{[f_X(x)]^2} \times \frac{f_X(x)}{F^{(1,1)}(x, z)} \Big|_{z=\xi_\alpha(x)} \\ &= \frac{F^{(1,0)}(x, z)f'_X(x) - F^{(2,0)}(x, z)f_X(x)}{f_{X,Z}(x, z)f_X(x)} \Big|_{z=\xi_\alpha(x)}\end{aligned}\quad (21)$$

where $f_X(x)$ is the marginal p.d.f. of X and $f_{X,Z}(x, z)$ is the joint p.d.f. of (X, Z) .

Applying the same method to the estimator, we have

$$\begin{aligned}\tilde{\xi}'_\alpha(x) &= \frac{\sum_{i=1}^n H(\frac{z-Z_i}{h})K(\frac{x-X_i}{h}) \sum_{i=1}^n K'(\frac{x-X_i}{h}) - \sum_{i=1}^n H(\frac{z-Z_i}{h})K'(\frac{x-X_i}{h}) \sum_{i=1}^n K(\frac{x-X_i}{h})}{\sum_{i=1}^n K(\frac{z-Z_i}{h})K(\frac{x-X_i}{h}) \sum_{i=1}^n K(\frac{x-X_i}{h})} \Big|_{z=\tilde{\xi}_\alpha(x)} \\ &= \frac{\tilde{F}^{(1,0)}(x, z)\tilde{f}'_X(x) - \tilde{F}^{(2,0)}(x, z)\tilde{f}_X(x)}{\tilde{f}_{X,Z}(x, z)\tilde{f}_X(x)} \Big|_{z=\tilde{\xi}_\alpha(x)},\end{aligned}\quad (22)$$

where

$$\begin{aligned}\tilde{F}^{(2,0)}(x, z) &:= \frac{1}{nh^2} \sum_{i=1}^n H(\frac{z-Z_i}{h})K'(\frac{x-X_i}{h}) \\ \tilde{F}^{(1,0)}(x, z) &:= \frac{1}{nh} \sum_{i=1}^n H(\frac{z-Z_i}{h})K(\frac{x-X_i}{h}) \\ \tilde{f}_{X,Z}(x, z) &:= \frac{1}{nh^2} \sum_{i=1}^n K(\frac{x-X_i}{h})K(\frac{z-Z_i}{h}) \\ \tilde{f}'_X(x) &:= \frac{1}{nh^2} \sum_{i=1}^n K'(\frac{x-X_i}{h}) \\ \tilde{f}_X(x) &:= \frac{1}{nh} \sum_{i=1}^n K(\frac{x-X_i}{h})\end{aligned}$$

Lemma: Under the conditions of Theorem 1, we have

1. $\sup_{x \in \mathcal{J}} |f_X(x) - \tilde{f}_X(x)| = o_p(1)$
2. $\sup_{x \in \mathcal{J}} |f'_X(x) - \tilde{f}'_X(x)| = o_p(1)$
3. $\sup_{x \in \mathcal{J}} \sup_{z \in \mathcal{Z}} |f_{X,Z}(x, z) - \tilde{f}_{X,Z}(x, z)| = o_p(1)$
4. $\sup_{x \in \mathcal{J}} \sup_{z \in \mathcal{Z}} |F^{(1,0)}(x, z) - \tilde{F}^{(1,0)}(x, z)| = o_p(1)$

$$5. \sup_{x \in \mathcal{J}} \sup_{z \in \mathcal{Z}} |F^{(2,0)}(x, z) - \tilde{F}^{(2,0)}(x, z)| = o_p(1)$$

Proof of Lemma: Items (1) - (3) follow immediately from Hansen (2008), while (4) follows from Samanta (1989). Proving (5) involves only a slight modification of the proof to (4).

Next, define the numerator in (21) as

$$p(x, z) := F^{(1,0)}(x, z)f'_X(x) - F^{(2,0)}(x, z)f_X(x)$$

and similarly from (22) define

$$\tilde{p}(x, z) := \tilde{F}^{(1,0)}(x, z)\tilde{f}'_X(x) - \tilde{F}^{(2,0)}(x, z)\tilde{f}_X(x).$$

Also define these denominators as

$$q(x, z) := f_{X,Z}(x, z)f_X(x)$$

$$\tilde{q}(x, z) := \tilde{f}_{X,Z}(x, z)\tilde{f}_X(x).$$

The lemma implies that

$$\sup_{x \in \mathcal{J}} \sup_{z \in \mathcal{Z}} |p(x, z) - \tilde{p}(x, z)| = o_p(1)$$

$$\sup_{x \in \mathcal{J}} \sup_{z \in \mathcal{Z}} |q(x, z) - \tilde{q}(x, z)| = o_p(1).$$

Next write

$$\tilde{\xi}'_\alpha(x) = \frac{\tilde{p}(x, \tilde{\xi}_\alpha(x))/q(x, \tilde{\xi}_\alpha(x))}{\tilde{q}(x, \tilde{\xi}_\alpha(x))/q(x, \tilde{\xi}_\alpha(x))},$$

and note that the lemma implies that

$$\begin{aligned} \sup_{x \in \mathcal{J}} \sup_{z \in \mathcal{Z}} \left| \frac{\tilde{q}(x, z)}{q(x, z)} - 1 \right| &= \sup_{x \in \mathcal{J}} \sup_{z \in \mathcal{Z}} \left| \frac{\tilde{q}(x, z) - q(x, z)}{q(x, z)} \right| \\ &\leq \frac{\sup_{x \in \mathcal{J}} \sup_{z \in \mathcal{Z}} |\tilde{q}(x, z) - q(x, z)|}{m_1 m_2} = o_p(1). \end{aligned}$$

Now

$$\sup_{x \in \mathcal{J}} \sup_{z \in \mathcal{Z}} \left| \frac{\tilde{p}(x, z)}{q(x, z)} - \frac{p(x, z)}{q(x, z)} \right| = \sup_{x \in \mathcal{J}} \sup_{z \in \mathcal{Z}} \left| \frac{\tilde{p}(x, z) - p(x, z)}{q(x, z)} \right| = o_p(1).$$

Since $\frac{\tilde{p}(x, z)}{q(x, z)}|_{z=\tilde{\xi}_\alpha(x)} = \tilde{\xi}'_\alpha(x)$ and $\frac{p(x, z)}{q(x, z)}|_{z=\xi_\alpha(x)} = \xi'_\alpha(x)$, we have that

$$\tilde{\xi}'_\alpha(x) = \xi'_\alpha(x) + o_p(1),$$

uniformly in x .

Proof of Theorem 2: First we discuss the existence of unique solutions to the equations

$$\frac{dz_{\alpha, x}(s)}{ds} = \xi_\alpha(z_{\alpha, x}(s)), \quad z_{\alpha, x}(0) = x \quad (23)$$

and

$$\frac{d\tilde{z}_{\alpha, x}(s)}{ds} = \tilde{\xi}_\alpha(\tilde{z}_{\alpha, x}(s)), \quad \tilde{z}_{\alpha, x}(0) = x. \quad (24)$$

for $s \in \mathcal{T} = [0, T_1]$ for some $0 < T_1 < \infty$. By the assumptions of the theorem, we have that the functions ξ_α and $\tilde{\xi}_\alpha$ are continuously differentiable over \mathcal{J} . It is well known that under these conditions that unique solutions exist to both (23) and (24).

As we are interested in the quantity $\sup_{s \in \mathcal{T}} |\tilde{\psi}(s) - z_{\alpha, x}(s)|$, that is, the supremum difference between the target and its estimate using $\tilde{\xi}_\alpha$ and some integration procedure, we have

$$\begin{aligned} \sup_{s \in \mathcal{T}} |\tilde{\psi}(s) - z_{\alpha, x}(s)| &\leq \sup_{s \in \mathcal{T}} |\tilde{\psi}(s) - \tilde{z}_{\alpha, x}(s)| + \sup_{s \in \mathcal{T}} |\tilde{z}_{\alpha, x}(s) - z_{\alpha, x}(s)| \\ &= S_1 + S_2 \end{aligned} \quad (25)$$

The quantity S_1 can be taken care of by the fact that $\tilde{\psi}$ is the numerical approximation of $\tilde{z}_{\alpha, x}$. Since the integration procedure is assumed to be of order q , it follows that $S_1 = O(\delta_n^q)$ (see the proof of the theorem in Abramson and Müller (1994)).

As for S_2 , consider a sequence of m starting points $s_i = \frac{(i-1)T_1}{m}$ for $i = 1, \dots, m$ and the following initial value problems with different starting levels:

$$\begin{aligned} \frac{dz_{\alpha,x}(s)}{ds} &= \xi_\alpha(z_{\alpha,x}(s)), & z_{\alpha,x}(s_i) &= z_{i1}, & s &\geq s_i \\ \frac{dz_{\alpha,x}(s)}{ds} &= \xi_\alpha(z_{\alpha,x}(s)), & z_{\alpha,x}(s_i) &= z_{i2}, & s &\geq s_i \end{aligned} \quad (26)$$

Denote the solutions to these equations as $z_{\alpha,x}(s; z_{i1})$ and $z_{\alpha,x}(s; z_{i2})$, respectively. These solutions depend continuously on the initial conditions z_{i1} and z_{i2} and so there exists a constant $C_1 > 0$ such that

$$|z_{\alpha,x}(s_{i+1}; z_{i1}) - z_{\alpha,x}(s_{i+1}; z_{i2})| \leq C_1 |z_{i1} - z_{i2}| \quad (27)$$

for $i = 1, \dots, m$. This controls the difference between two solutions with different initial conditions. Next consider a third initial value problem

$$\frac{d\tilde{z}_{\alpha,x}(s)}{ds} = \tilde{\xi}_\alpha(\tilde{z}_{\alpha,x}(s)), \quad \tilde{z}_{\alpha,x}(s_i) = \tilde{z}_i \quad s \geq s_i, \quad (28)$$

and denote the solution to this equation as $\tilde{z}_{\alpha,x}(s; \tilde{z}_i)$. Next we bound the quantity

$$\sup_{s_i \leq s \leq s_{i+1}} |z_{\alpha,x}(s; \tilde{z}_i) - \tilde{z}_{\alpha,x}(s; \tilde{z}_i)|.$$

By making use of a Taylor expansion, and noting that at the starting time s_i , the two functions $z_{\alpha,x}$ and $\tilde{z}_{\alpha,x}$ are the same at \tilde{z}_i , we have that

$$\begin{aligned} z_{\alpha,x}(s; \tilde{z}_i) - \tilde{z}_{\alpha,x}(s; \tilde{z}_i) &= z_{\alpha,x}(s_i; \tilde{z}_i) - \tilde{z}_{\alpha,x}(s_i; \tilde{z}_i) \\ &\quad + (s - s_i)(z'_{\alpha,x}(s_i; \tilde{z}_i) - \tilde{z}'_{\alpha,x}(s_i; \tilde{z}_i)) \\ &\quad + \frac{(s - s_i)^2}{2}(z''_{\alpha,x}(\zeta; \tilde{z}_i) - \tilde{z}''_{\alpha,x}(\zeta; \tilde{z}_i)), \end{aligned}$$

for some $\zeta \in (s_i, s)$, which leads to

$$\sup_{s_i \leq s \leq s_{i+1}} |z_{\alpha,x}(s; \tilde{z}_i) - \tilde{z}_{\alpha,x}(s; \tilde{z}_i)| \leq \frac{C_2}{m} |\xi_\alpha(\tilde{z}_i) - \tilde{\xi}_\alpha(\tilde{z}_i)| + \frac{C_3}{m^2} (C_4 + \sup_{x \in \mathcal{J}} |\xi'_\alpha(x) - \tilde{\xi}'_\alpha(x)|), \quad (29)$$

for $0 \leq i \leq m$ and constants $C_2, C_3, C_4 > 0$.

Now we have a way of controlling the difference between two different solutions given the same initial condition. We can put this together with (27) to get an overall upper bound. First notice that for $s \geq s_i$, we have

$$\begin{aligned} \tilde{z}_{\alpha,x}(s) &= \tilde{z}_{\alpha,x}(s; \tilde{z}_{\alpha,x}(s_i)) \\ z_{\alpha,x}(s) &= z_{\alpha,x}(s; z_{\alpha,x}(s_i)). \end{aligned} \quad (30)$$

Then for $0 \leq i \leq m$, we have

$$\begin{aligned} \sup_{s_i \leq s \leq s_{i+1}} |z_{\alpha,x}(s) - \tilde{z}_{\alpha,x}(s)| &\leq \sup_{s_i \leq s \leq s_{i+1}} |\tilde{z}_{\alpha,x}(s; \tilde{z}_{\alpha,x}(s_i)) - z_{\alpha,x}(s; \tilde{z}_{\alpha,x}(s_i))| \\ &\quad + \sup_{s_i \leq s \leq s_{i+1}} |z_{\alpha,x}(s; z_{\alpha,x}(s_i)) - z_{\alpha,x}(s; \tilde{z}_{\alpha,x}(s_i))| \\ &\leq O_p\left(\frac{\beta_n}{m}\right) + C_1 |z_{\alpha,x}(s_i) - \tilde{z}_{\alpha,x}(s_i)|, \end{aligned} \quad (31)$$

where the O_p terms are uniform in i . If we choose $m = n$, then it follows that

$$|\tilde{z}_{\alpha,x}(s_{i+1}) - z_{\alpha,x}(s_{i+1})| \leq O_p\left(\frac{\beta_n}{n}\right) + C_1 |z_{\alpha,x}(s_i) - \tilde{z}_{\alpha,x}(s_i)|.$$

Since the two functions $z_{\alpha,x}$ and $\tilde{z}_{\alpha,x}$ have the same initial condition of x at time $s_0 = 0$, we have

$$\sup_{1 \leq i \leq n} |\tilde{z}_{\alpha,x}(s_i) - z_{\alpha,x}(s_i)| = O_p(\beta_n),$$

and therefore

$$\sup_{s_i \leq s \leq s_{i+1}} |\tilde{z}_{\alpha,x}(s) - z_{\alpha,x}(s)| = O_p(\beta_n),$$

which, since this result is uniform in i , implies

$$\sup_{s \in \mathcal{T}} |\tilde{z}_{\alpha,x}(s) - z_{\alpha,x}(s)| = O_p(\beta_n).$$

SUPPLEMENT: ADDITIONAL MATERIALS

Sample Size	α	Logistic Model	Kernel Smoothing	Joint Kernel
300	.05	1.66	.927	1.74
	.25	6.06	2.25	2.30
	.50	3.18	1.65	1.66
	.75	.845	.751	.830
	.95	2.37	.476	.501
1000	.05	1.56	.644	.671
	.25	6.11	1.62	1.61
	.50	3.24	1.18	1.23
	.75	.862	.632	.658
	.95	2.48	.541	.542

Table 2: AISE scores ($\times 0.1$) for various scenarios in the quadratic simulation study, each with a starting value of $x = 180$.

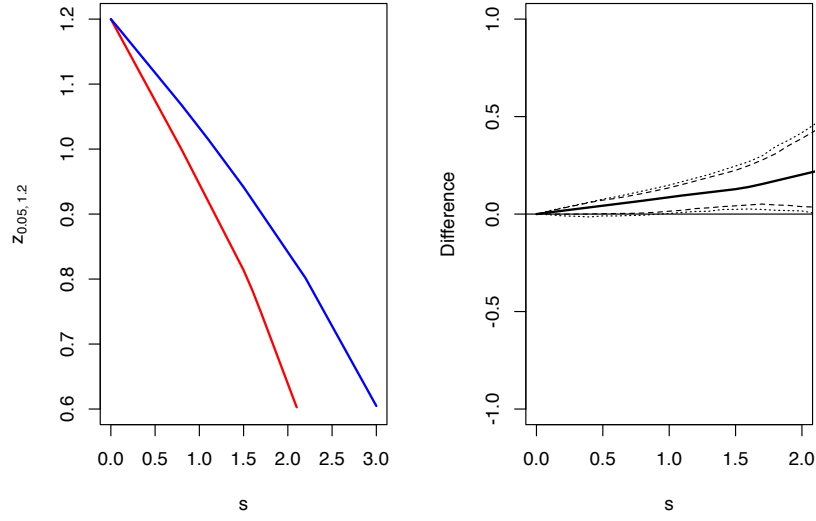


Figure 12: A low quantile comparison between normal and impaired subjects starting from $x = 1.2$. Here $\alpha = .05$

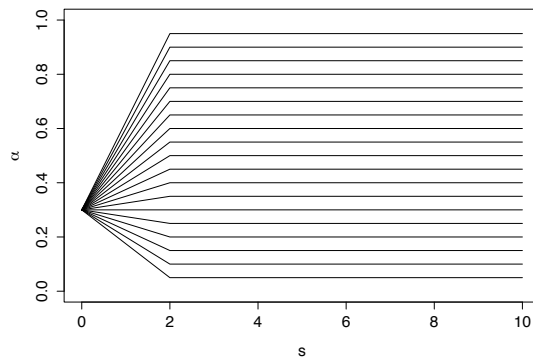


Figure 13: A demonstration of $\alpha(s)$ for $\alpha \in \{.05, \dots, .95\}$, starting from $\alpha^* = 0.3$ and with $S^* = 2$.